Vanadium MXenes materials for next-generation energy storage devices

IOP Publishing Nanotechnology
Nanotechnology 34 (2023) 252001 (16pp) https://doi.org/10.1088/1361-6528/acc539

Topical Review

Vanadium MXenes materials for next-generation energy storage devices

Ayomide Adeola Sijuade[1], Vincent Obiozo Eze[1], Natalie Y Arnett[1] and Okenwa I Okoli[1,2,*]

[1] High-Performance Materials Institute, FAMU-FSU College of Engineering, Tallahassee, FL 32310, United States of America
[2] Herff College of Engineering, University of Memphis, Memphis, TN, 38111, United States of America

E-mail: okoli@eng.famu.fsu.edu

Received 30 September 2022, revised 12 December 2022
Accepted for publication 17 March 2023
Published 11 April 2023

Abstract

Batteries and supercapacitors have emerged as promising candidates for next-generation energy storage technologies. The rapid development of new two-dimensional (2D) electrode materials indicates a new era in energy storage devices. MXenes are a new type of layered 2D transition metal carbides, nitrides, or carbonitrides that have drawn much attention because of their excellent electrical conductivity, electrochemical and hydrophilic properties, large surface area, and attractive topological structure. This review focuses on various synthesis methods to prepare vanadium carbide MXenes with and without etchants like hydrofluoric acid, lithium fluoride, and hydrochloric acid to remove the 'A' layers of the MAX phase. The goal is to demonstrate the utilization of a less toxic etching method to achieve MXenes of comparable properties to those prepared by traditional methods. The influence of intercalation on the effect of high interlayer spacing between the MXene layers and the performance of MXenes as supercapacitor and battery electrodes is also addressed in this review. Lastly, the gaps in the current knowledge for vanadium carbide MXenes in synthesis, scalability, and utilization in more energy storage devices were discussed.

Keywords: 2D materials, transition-metal carbide, MXene, synthesis, batteries, supercapacitors

(Some figures may appear in colour only in the online journal)

1. Introduction

Humanity's survival depends on efficiently producing, storing, and utilizing the available fuels needed for energy production in an environmentally benign manner [1, 2]. The increasing use and demand for energy in association with the issues related to global warming and the depletion of fossil fuels have encouraged the switch to alternative and reliable sources of energy and energy storage devices [3]. This issue has resulted in seeking effective methods for developing advanced catalysts and electrode materials [4] utilized in energy storage devices like batteries [5], capacitors [6], and supercapacitors [7]. Nonetheless, the upscale of the following energy generation and storage materials depends on the production costs, stability, efficiency, and safety of the various electrode materials used in their manufacture. The most efficient electrode materials tested are noble metals like ruthenium, iridium, platinum, and their composites; however, severe limitations in the practical day-to-day application of the metals still exists due to their high cost and scarcity [8–12].

Over the years, alternative research on micro and nanomaterials as electrode materials has attracted much attention. These materials are characterized to allow for easy electron transport, high surface area, increased rate of reaction, and better intercalation strain accommodation [13]. The utilization of lithium-ion [14] and alkaline [15] batteries have led to a tremendous breakthrough in energy storage devices. However, the inherent limits of these micro and nanomaterials have failed to meet the ever-rising electricity needs.

* Author to whom any correspondence should be addressed.

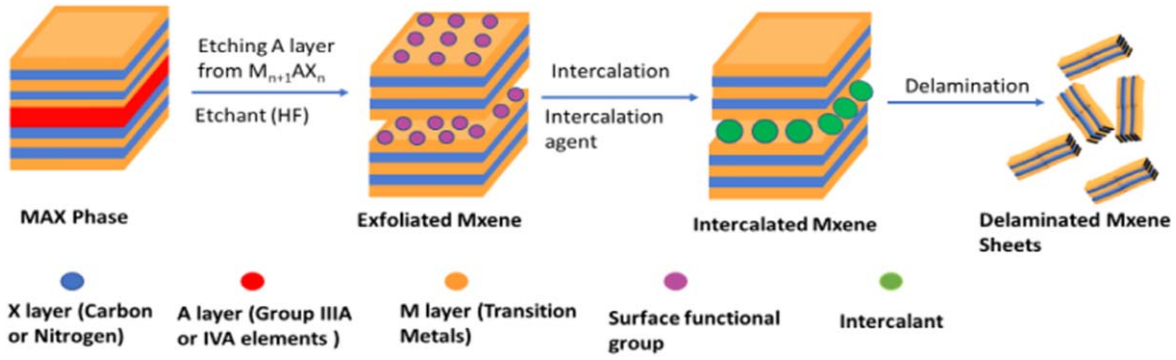

Figure 1. Schematic diagram of MXene synthesis from MAX phase.

Micromaterials' intrinsic properties and single-phase nanomaterial's weak mechanical stability, low conductivity, and unwanted side reactions have disadvantaged these batteries from fulfilling the energy requirements [16–18]. The continuous search for highly active, low-cost, and stable materials with exceptional charge transfer efficiency has led to numerous carbon-based derivatives [19], conducting polymers, and metal oxides discovery. These include carbon nanotubes [20], graphene [21], magnesium oxide [22], activated carbon [23], and ruthenium oxide [24].

Although carbon presents as a widely used cheap, non-toxic material with a large specific area and an easy synthesis route, when activated, its capacitance is hindered by the various pore sizes gotten during the process. This limits its energy density, conductivity, and capacitance by impeding ion passage across a particle in supercapacitors [18, 25–27]. A good example is graphene, with a high theoretical specific surface area of 2630 $m^2\ g^{-1}$ while only reaching an actual capacitance of 330 F g^{-1}. This can be attributed to the irreversible self-stacking and the clustering of graphene sheets during the electrochemical and electrode fabrication process [28].

Ruthenium oxide has good electrical conductivity, mechanical strength, frequency response, and stability but has a high fabrication cost [26, 29]. To improve the cost-effectiveness, Han *et al* fabricated RuO_2-coated vertical graphene hybrid electrodes for supercapacitors with an aerial capacitance of 2143 F g^{-1} [29]. However, ruthenium remains an expensive precursor for electrode materials. The high cost of ruthenium oxide has opened doors for alternatives such as magnesium oxide (MgO) as electrode materials. Feng *et al* reported MgO's excellent cycling capability with a capacity retention rate of almost 100% after 10000 cycles. On the other hand, graphene is a good conductor of electricity and heat and is extremely lightweight and robust [21]. However, the graphene layers get clustered easily, inhibiting the free flow of electrolyte ions [30].

Research into improving the physical and chemical properties of 2D materials led to the discovery of the first MXenes $Ti_3C_2T_x$ in 2011 by Gogotsi and coworkers [31]. MXenes have been called wonder materials due to their unique microstructures and abundant surface terminations resulting in fantastic electrical, mechanical, and thermal properties [32]. V_2C MXenes are stable at 150°C in air and temperatures up to 375°C in an argon atmosphere. However, the V_2C MXene oxidizes with a temperature increase to form nanoparticles containing vanadium trioxide V_2O_3 and vanadium carbide V_8C_7 [33]. MXene flakes have the formula $M_{n+1}X_nT_x$ (n=1, 2, or 3), where M stands for early transition metals interwoven with carbon or nitrogen layers (X). Figure 1 shows a schematic illustration of a typical MXene synthesis process with an acid exfoliant. As shown in figure 1, the selective etching of A layers (group IIIA or IVA elements like Al and Si) from the MAX phase results in the synthesis of MXenes. The MAX phase comes from a family of ternary carbides and nitrides with the formula $M_{n+1}AX_n$ ($n = 1, 2, 3$), with M and X being the same as MXenes but A layers representing an element from group IIIA or IVA [34–36]. Depending on the synthesis method, the T_x represents the different functional groups like hydroxyl, oxygen, or fluorine [37–40]. Density functional theory calculations predicted that MXenes with OH, O, or F terminations are semiconductors with a bandgap range of 0.05–1.8 eV. Whereas bare MXenes are predicted to be metallic conductors [41]. Due to the diversity of transition metals that MXenes possess, around 30 types are reported, and about 70 are theoretically projected. MXenes applications include wearable sensors, nuclear waste treatment, gas sensors, hydrogen storage, photocatalysis, batteries, and hydrogels [42–47]. Much research has gone into using MXenes for energy storage devices due to their excellent conductivity, large surface areas, environment-friendly nature, and good rate capabilities [48].

Vanadium carbide MXenes (V_2C) are fascinating due to their lightweight, pseudocapacitive behavior, high Li-ion intercalation capacity, and conductivity [49, 50]. Vanadium MXenes also have a greater interlayer spacing than as-prepared Ti- and Mo-based MXenes, which is advantageous for energy storage intercalation and deintercalation [51]. In addition, the various valence states of +2, +3, and +4 of the vanadium MXenes have proven advantageous for electrochemical performance as supercapacitor electrodes [52]. This paper focuses on the review of V_2C MXenes, the synthesis, structure, properties, applications in energy storage devices, and the issues with commercializing their use.

2. Synthesis of vanadium carbide MXenes

MXene synthesis involves the selective etching of the A layers of the MAX phase precursors (figure 1). There are two bonds in

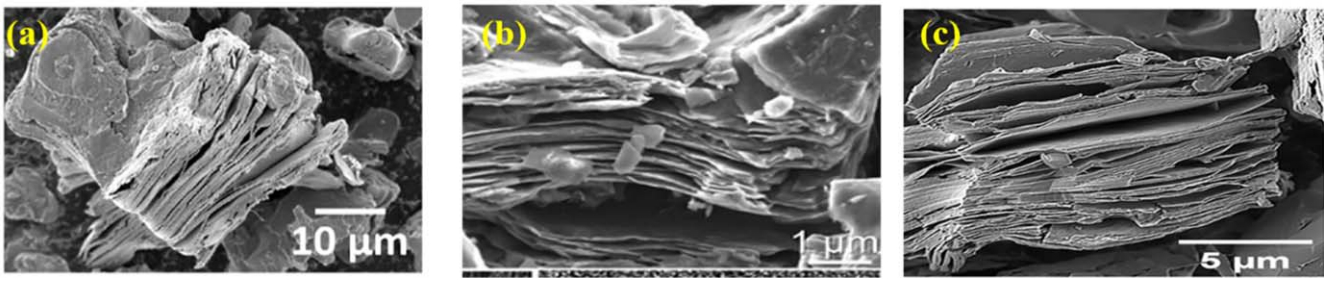

Figure 2. SEM images of V_2CT_x MXene etched with HF by (a) Reprinted (adapted) with permission from [43]. Copyright (2019) American Chemical Society. (b) Reprinted (adapted) with permission from [41]. Copyright (2013) American Chemical Society. (c) VahidMohammadi *et al* Reprinted (adapted) with permission from [59]. Copyright (2017) American Chemical Society.

MAX phase structures: the M–X and M–A bond. Due to the strong bond between the M–X layers, separating them through mechanical shearing is difficult. However, the M–A bonds can be separated through selective etching of A layers due to their chemical activity, which is critical in making MXenes [53]. It is also important to note that etching is a kinetically controlled process; therefore, each MXene needs different reaction times and temperatures to complete conversion depending on the MAX phase [53–56]. Typically, MXenes with larger n in $M_{n+1}C_nT_x$ translate to a more significant number of transition metals and carbon atoms needing stronger etching or longer duration. An example is $Mo_2Ti_2AlC_3$ ($n = 3$) which requires an etching time double its counterpart Mo_2TiAlC_2 ($n = 2$) under the same etching conditions [53], and $V_4C_3T_x$, which requires an etching time of 96 h compared to the V_2CT_x etched for 8 h [46, 48]. In addition, the synthesis method adopted determines the position of the peaks, which depends on the amount of trapped water between the MXene layers. V_2C MXene synthesis has been explored through various methods, including etching with HF [43], NaF [33], LiF [57], and electrochemical etching [58].

2.1. Hydrogen-fluoride etching

The first successful etching of V_2CT_x was done by Naguib *et al* [41] using HF on V_2AlC, they achieved a yield of 90% after etching for 9 h. Since then, other researchers have successfully synthesized V_2CT_x with HF and have used it for hydrogen evolution, batteries and gas sensors [43, 59, 60]. The V_2C MXenes synthesized with this method are usually multilayered, accordion-like structures with XRD peaks corresponding to (0002) planes [41, 43, 59]. Figure 2 shows the SEM image similarities of V_2C MXenes synthesized with the HF method. Using atomic force microscopy (AFM), Lee *et al* found that the single-layer flakes had a thickness of ∼1.75 nm after delamination [43], which correlates to ∼1 nm reported by Naguib *et al* and a yield of 60% [41]. HF is highly selective and has good etching qualities, so much so that it can selectively etch cubic SiC. This process can be upscaled to manufacture nanodevices such as cellular probes and sensors [61, 62]. However, HF's acute toxicity prevents the large-scale synthesis of MXenes through this method and, ultimately, the comprehensive utilization of MXenes in energy-related applications [58]. Also, high levels of HF can significantly irritate the eyes, skin, and nasal passages. Lastly, high concentrations may infiltrate the lungs and result in excessive bleeding and edema. To prevent these issues, other methods of MXene synthesis are explored.

2.2. Hydrogen-fluoride free etching

2.2.1. Etching with fluoride salts. As an alternative to etching V_2CT_x with HF, strong acid and a fluoride salt can be used to form *in situ* HF that etches the A layers [53]. Guan *et al* demonstrated the good etching ability of LiF + HCl for 120 h to produce uniform multilayered, high-purity MXene sheets [57]. TEM images in figure 3 reveals that the distance between the parallel planes of the MXene sheets (*d*-spacing) is about 0.97 nm. It was also observed that the MXenes have large and thin flakes with no pores or particles found on the surface, consistent with the V_2C MXenes etched in KF + HCl, $(NH_4)HF_2$, and NaF + HCl solutions [57]. Wu *et al* found that NaF + HCl is the most efficient fluoride salt used in etching compared to LiF + HCl, NaF + HCl, and KF + HCl [33]. After etching with HCl and NaF, Liu *et al* discovered that etching with fluoride salts results in purer MXenes due to the intensity ratio of V_2AlC's (002) peak to V_2C's (002) peak (I_{MAX}/I_{MXene}) value of 4.11% [63]. This result indicates that more MXenes were converted from the MAX phase using NaF + HCl as there was a decrease in the ratio of the MAX phase to MXene after 72 h, making NaF + HCl better than any other method of etching. SEM images of the synthesized MXenes reveal a quasi-2D structure with thin layers, as shown in figure 3(c) [63]. It is important to note that different fluoride salts require unique etching times (120 h for LiF + HCl etching and 72 h for NaF + HCl etching) [46, 51]. The molten salt environment also provides a viable and green chemistry for the synthesis of MXenes [64]. The traditional MXene phases can also be synthesized with Molten $ZnCl_2$. The Cl- terminated MXenes are expected to be more stable than the F-terminated MXenes which should improve the energy storage applications. However, V_2CCl, could not be synthesized due to the higher M–A bonding strengths than Ti_3ZnC_2, and Ti_2ZnC [64]. The equation for the reaction is proposed below;

$$V_2AlC + 3ZnCl = V_2C + 3Zn + AlCl_3. \quad (1)$$

2.2.2. Electrochemical etching. Electrochemical etching (E-etching) resolves the issues associated with HF toxicity. Herein, V_2CT_x was etched using 0.4 V to 0.7 V to create the

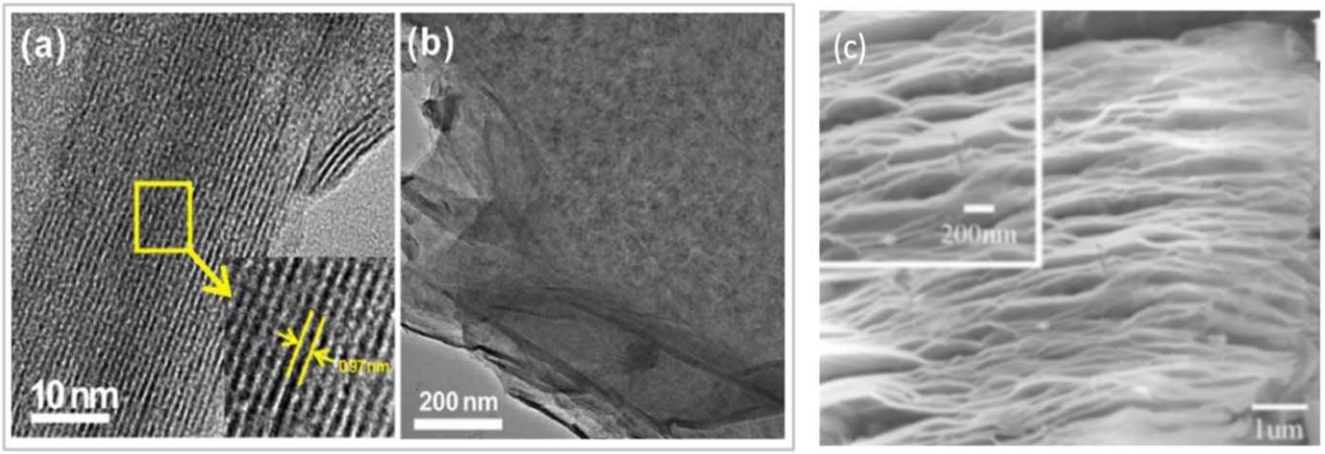

Figure 3. (a), (b) TEM images of V_2C etched with HCl and LiF. Reproduced from [57]. © IOP Publishing Ltd. All rights reserved. (c) SEM image of V_2C after 72 h. Reproduced from [63]. © IOP Publishing Ltd. All rights reserved.

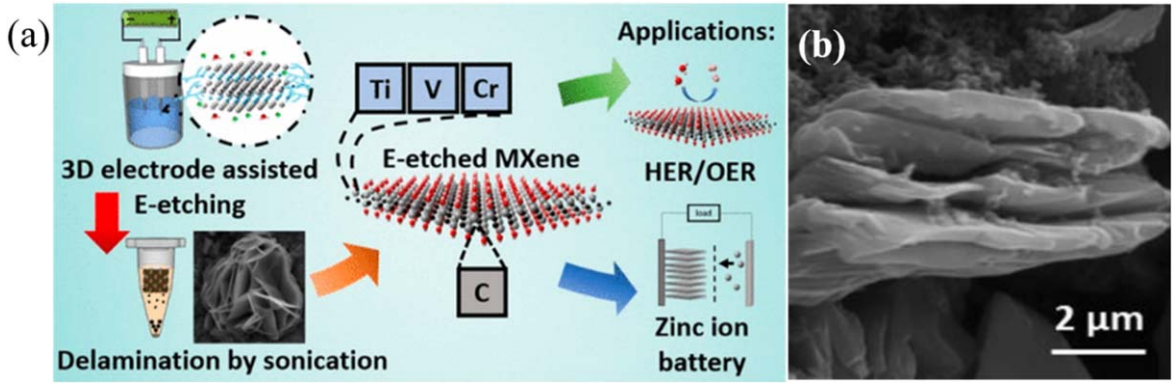

Figure 4. (a) Electro-etching method and the applications (b) V_2CT_x synthesized with electrochemical etching. Reprinted (adapted) with permission from [58]. Copyright (2019) American Chemical Society.

MXene under fixed conditions of (1 M/50 °C) for 9 h as seen in figure 4(a). The optimized voltage for etching was 0.5 V resulting in V_2CT_x MXenes with a micro-size of 25 μm and a flower-like architecture. The synthesized MXene exhibited a specific capacity of 100 mhA g^{-1} [58]. Figure 4(b) shows the layered MXene structure achieved after synthesis depicting the accordion-like structure with a lateral size of >1 μm and thickness of 5–80 nm. It was also noticed that MXenes E-etched had substrate-driven architectures and can be very useful for forming various 3D composites [58]. However, lower yields (~50%) and residual MAX precursors were obtained from the E-etched method, uncharacteristic of other solvent-based methods. Since the by-products from this method can be recycled, the yield can be improved by recycling the sediments of the MAX phase, which can increase the conversion rate to ~75% [58].

2.2.3. NH_4HF_2 etching. Another method to reduce the toxicity of HF is replacing it with relatively mild NH_4HF_2 [65]. The etching reactions are shown in equations (2) and (3) below [2];

$$M_{n+1}AX_n + 3NH_4HF_2 = (NH_4)AlF_6 + 3/2H_2 + M_{n+1}X_n \quad (2)$$

$$M_{n+1}X_n + aNH_4HF_2 + bH_2O = (NH_3)_C(NH_4)_dM_{n+1}X_n(OH)_XF_y. \quad (3)$$

This method does not require a delamination step as NH^{4+} is inserted between the MXene nanosheet layers which increases the interlayer spacing [2]. Feng *et al* synthesized Ti_3C_2 MXenes using NH_4HF_2 to obtain larger interlayer spacing, improving the space for ion-embedded Ti_3C_2 to be stored. The MXenes were synthesized by adding 1g Ti_3AlC_2 to NH_4HF_2 and were stirred at 60°C. The etched products were then washed in deionized water until a neutral pH was reached. From the results, Ti_3C_2 etched with NH_4HF_2 had better pseudo capacitance with a specific capacitance of 78 F g^{-1}[66]. Even though NH_4HF_2 has been used to synthesize titanium-based MXenes, its utilization is lacking for vanadium-based MXenes to the best of the writer's knowledge. Further research is required to develop this synthesis process for vanadium-based MXenes.

2.3. Delamination

After synthesis, delamination of the MXene layers is significant because the resulting layers are held together by Van

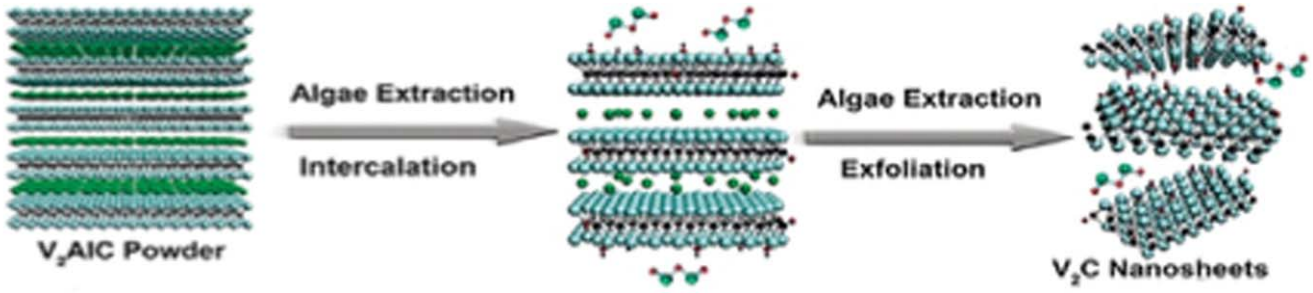

Figure 5. Schematic diagram of V_2C by algae extraction from Zada *et al* Reproduced from [68] with permission from WILEY-VCH, copyright 2020.

Table 1. Yield, particle size, and applications of MXenes synthesized with different methods.

	Vanadium carbide MXenes			Titanium carbide MXenes			
Method of synthesis	Yield	Particle size	Etching time (hours)	Yield	Particle size	Etching time (hours)	References
HF etching	60%	< 1 μm	8	80%	2 μm	10	[41, 69]
LiF + HCl	91.3%	<1 μm	120	$\sim$100%	$\sim$1 μm	10	[57, 70]
NaF + HCl	$> 90\%$	<1 μm	72	84%	2 μm	48	[63, 71]
KF + HCl	No yield	No yield	—	87%	11.8 μm	3	[33, 72]
Electrochemical etching	50%	25 μm	9	>90%	18.6 μm	9	[58, 73]
I, Br +HCl	N/A	N/A	—	71%	1.8 μm	—	[74]

der Waals or hydrogen bonds, preventing the single flakes from forming. Delamination/exfoliation subjects the MXene layers to further treatment, allowing the formation of single flake MXene layers. First, the MXenes are intercalated with ionic or organic molecules and/or inorganic cations, followed by handshaking or ultrasonication for a while. Naguib *et al* investigated the intercalation of vanadium carbide (VC) MXenes with tetrabutylammonium hydroxide (TBAOH). It showed that a peak shift and an overall decrease in the *d*-spacing occurred, which confirms the delamination of the MXenes [67]. Other compounds like choline hydroxide and n-butylamine also successfully delaminated the MXene sheets [67]. Zada *et al* explored green delamination using algae. Figure 5 shows the synthesis procedure of the delaminated MXene sheets using the algae extraction approach. The delamination resulted in MXene sheets with good structural stability, a high absorption rate, and a yield of 90% [68]. Based on the above-discussed MXene synthesis methods, table 1 below compares the yield, particle size, and etching time for different synthesis methods for titanium and vanadium MXenes.

2.4. Solid-solution MXenes

A class of double transition metal (DTM) MXenes was discovered in 2015 by combining two transition metals in an ordered structure. This entailed sandwiching one or two layers of a transition metal (M') between two layers of another transition metal (M') [75]. These phases exhibit out-of-plane ordering in M_3C_2 and M_4C_3 MXenes and have been computationally predicted to be stable [75]. However, not many have been synthesized or characterized, some of which include Mo_2TiC_2 and $Mo_2Ti_2C_3$ [76, 77] with even fewer studies done on DTM with randomly mixed transition metal atom (solid solutions) [75]. Studies have predicted that DTM structures would result in a modification of the electronic state of the metal layers, improve electrical conductivity, and catalytic activity or pseudo-capacitive charge storage [78]. Single-phase V_2CT_x has been studied as electrodes in supercapacitors, lithium-ion, zinc-ion, and aluminum-ion batteries. However, the electrochemical properties of solid-solution MXenes are less known with M_2XT_x not reported [79].

Wang *et al* synthesized two series of niobium-containing solid-solution MXenes, $Ti_{2-y}Nb_yCT_x$ and $V_{2-y}Nb_yCT_x$ ($y = 0.4$, 0.8, 1.2, and 1.6), investigated their electrochemical properties and compared them to corresponding single-metal MXenes (Ti_2CT_x, Nb_2CT_x, and V_2CT_x) [79]. It was discovered that modifying the M-site chemistry tuned the capacitive behavior and cycling stability of the MXenes. Also, as the niobium content increased, the redox peak prominence decreased while the cycling stability was enhanced [79]. Another study by Wang *et al* [80] studied the performance of $V_3CrC_3T_x$ MXenes as anodes in Zn-ion supercapacitors. It was found that partially replacing Cr atoms for V atoms in $V_4C_3T_x$, caused an increase in the interlayer spacing of the MXenes, which in turn caused an increase in the adsorption of Zn ions and ion diffusion. This improved the capacitance, discharge potential and cycle stability of the

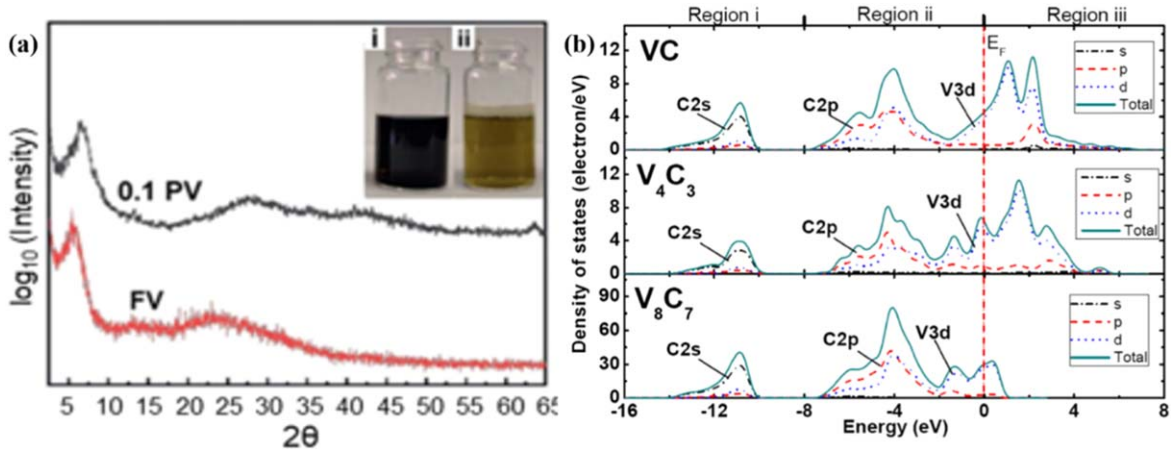

Figure 6. (a) XRD patterns of untreated- V_2CT_x (red) samples and 0.1 M polyphosphate-V_2CT_x (black). Pictures on the top right show (i) 0.1 M polyphosphate- V_2CT_x (left) sample and (ii) untreated V_2CT_x sample (right) after three weeks of exposure to ambient air. [84] John Wiley & Sons. [© 2019 Wiley-VCH Verlag GmbH & Co. KGaA, Weinheim]. (b) total density of states (TDOS) and partial density of state (PDOS) for VC, V_4C_3, and V_8C_7. Reproduced from [85]. © IOP Publishing Ltd. All rights reserved.

synthesized batteries. They also demonstrated outstanding mechanical flexibility with an ultra-high area energy density of 51.12 μW h cm^{-2}, long cycle life of 20 000 cycles (84.5% capacitance retention), and bendability of 10 000 cycles (80.2% capacitance retention) [80]. Different compositions of $Mo_xV_{4-x}C_3$ with $x = 1$, 1.5, 2, and 2.7 were synthesized by Pinto *et al* [75]. It was discovered that varying the Mo:V ratio, the electrical, electrochemical, and surface termination ratios (O:F ratio), can be tuned. The highest of these ratios was the $Mo_{2.7}V_{1.3}C_3$ composition which showed a volumetric capacitance of 860 F cm^{-3} and a high electrical conductivity of 830 S cm^{-1} at room temperature [75].

3. Structure and properties of vanadium carbide MXene that make them suitable for energy storage devices

V_2C MXenes have a closely packed structure before delamination, similar to their MAX phase precursors. The X atoms partially fill the octahedral vacancies of the face cubic center (fcc) sublattice, which makes them have structural deficiencies [47, 81]. The crystalline structure resembles the NaCl cubic structure, as seen in figure 6, with a disordered δ-VC_{1-x} ($VC_{0.65}$-$VC_{0.90}$) extensive homology. The high structural deficiencies make V_2C MXenes suitable for electronic applications [81]. The structural defects may lead to atomic ordering connected to the rearrangement of non-metallic atoms and structural vacancies at interstitial lattice positions. Shacklete *et al* showed that the resistivity of vanadium carbide in the disordered phase is increasingly higher than in the ordered phase due to the disordered phase transition [82]. Therefore, the ordered phase is more suitable for electrical and energy storage applications. This finding suggests that the ordering from the structural deficiencies found in vanadium carbide is highly significant. Theoretically, V-based and vanadium-containing MXenes have a higher electrochemical theoretical capacity than the popular $Ti_3C_2T_x$ MXenes in batteries. Realizing the high theoretical capacity depends on the high purity V_2C MXene; however, this is difficult to achieve. The difficulty of synthesis arises from the higher formation energy of V_2C from V_2AlC compared to other MXenes [63]. This high theoretical capacity might be due to vanadium's rich valence charges from +2 to +5. Due to the formation of structural vacancies in vanadium carbide and the unique ordering of the carbon atoms in its structure, V_2C MXenes are responsible for increasing microhardness and electrical conductivity [83].

Vanadium carbide has six solid single-phase zones: VC, α-V_2C, β-V_2C, V_4C_3, V_6C_5, and V_8C_7. Each of these has a different resistivity depending on the ordering. Because of their narrow band gaps, all vanadium carbides (VC) MXenes have metallic properties at the Fermi level. Although a covalent bond exists between the transition metal and carbon, V_2C MXenes also has metallic and ionic properties, resulting in a high melting point, good corrosion resistance, high hardness, and good electrical conductivity [82]. However, as demonstrated by other MXene types, V_2C MXenes are highly unstable due to the –OH, –O, or –F terminations formed due to the etching process.

Usually, oxidation starts at the edges and gets defective in the presence of oxygen and water [53]. This property strongly hinders practical use and warrants special storage conditions in dark, low-temperature, non-aqueous environments to prevent oxidation. In addition, edge binders may be used to increase the material's shelf life [86]. Iqbal *et al* revealed that using polyanionic salts, such as polyphosphates (P), polysilicates (Si), and polyborates (B) as edge binders drastically improved the shelf life of vanadium and titanium-based MxXnes [87]. In particular, the shelf life of V_2CT_x drastically improved with the use of polyphosphate [87]. Figure 6(a) shows the XRD patterns of V_2CT_x treated with 0.1 M polyphosphate(black) and untreated V_2CT_x. The XRD graphs show that the V_2CT_x synthesized with 0.1 M polyphosphate salt and stored under vacuum had the (002) and (110) peaks near 6° and 64°, respectively, which are

characteristic peaks of V_2CT_x. Also, no other peaks were observed, indicating that at the XRD level, neither case detected oxidation. However, no V_2CT_x diffraction peaks were obtained from the V_2CT_x with no added salt. This issue might be because of the dissolution of V_2CT_x due to the presence of V_2O_5. It can also be seen from figure 6(a) that there is a characteristic color difference between the sample with polyphosphate salt (figure 6(a) (i)) and without the polyphosphate salt (6a (ii)). The V_2CT_x suspension without the salt oxidizes and gives off the characteristic orange color of dissolved V^{5+} ions in the water. At the same time, the polyphosphate salt sample did not experience any color change compared to a new colloidal suspension [87]. Another study by Natu *et al* demonstrated polyanionic salts as edge binders to mitigate oxidation [84].

It was discovered that among the salts tested, polyphosphates, polyborates, and polysilicates, polyphosphates salts were the best at suppressing MXene oxidation for up to three weeks in the air, as illustrated. Additional advantages associated with polyanionic salts include low-cost and easy purification [84].

3.1. Intercalation mechanism in MXenes

Intercalation was first reported in 1957 by McDonnell *et al* without explaining how it works [88]. Over the years, research on intercalation has resulted in it being defined as the reversible uptake of guest molecules in chained or layered structures due to weak intercalation. During intercalation, the lattice swells, and the chain structure is not as stable as the layered structure, which may cause disintegration. A significant characteristic of intercalation is that the insertion of guest atoms does not change the lattice structure of the host and is usually highly mobile [86]. Intercalation reaction involves separating 2D layers and the addition of guest molecules. This process requires enough chemical driving force between host material layers and intercalants [89]. The thermodynamic principle for intercalation reactions is shown in equation (4). It is important to note that the energy involved in the process is affected by changes in the chemical structure and electrostatic states, the lateral size of the exposed boundaries, and the mechanics of the layered structures [90]

$$2\Delta G_f(\text{layer-intercalants}) - \Delta G_f\ (\text{layer-layer}) < 0. \quad (4)$$

For intercalation to happen in layered solids, the host layer and guest intercalants' energy levels or electron shells must match, which is controlled by the chemical structure. Three primary layered materials exist; graphite-like material dominated by Van der Waals gaps, TMD-like layered solids with polar covalent bonds and weak Van der Waals forces, and clay-like layered materials with high electron-negative elements on the surface. The (–O/–OH/–F) surface groups in clays exhibit high polarity, differentiating the intercalation method. MXenes have the following unique intercalation mechanisms: (i) The higher the polarity of the molecules, the more spontaneous the reaction (e.g. intercalation with dimethyl sulfoxide), (ii) When cations with high solvation enthalpy are inserted, it enables the co-intercalation of solvents as the ions would dissolve in the solvent (iii) electrically polarized MXene nanosheets aid in the electrochemical intercalation of ions species which is the mechanism for energy storage [86]. Figure 7 shows an example of the clay-like structure MXenes also displays [70].

These clay-like properties of MXenes allow flexible, free-standing films to be produced, molded and dried into conducting objects in any shape or conductive coating on a surface to be painted after dilution. Figure 7(b) and (c) depicts the cross-section and top view of the clay-like MXenes. After hydration, the dried samples swell and shrink after drying. Figure 7(d) shows the MXenes molded into the letter M and dried to form a conductive solid [70]. The intercalations usually occur as electrostatic interactions and coordination interactions with metal cations. MXenes have the exact intercalation mechanism as layered clay minerals based on similar layer rigidity and surface terminations. However, the layers in MXenes are fused more tightly, requiring stronger chemical interactions to drive the intercalation process [86].

3.2. Effect of the different valence charges of vanadium carbide MXenes

Initially, non-stoichiometric and stoichiometric VC were investigated due to differences observed in mechanical and thermal properties, including high thermal and electric conductivity, high melting point, and high-temperature, high-temperature hardness, and corrosion resistance [73, 74]. Some applications include corrosion protection and binders, microelectronics, thermal barriers, catalysts, and functional coatings [85]. Chong *et al* investigated the stability of V_2C, V_4C_3, V_6C_5, and V_8C_7. It was observed that the stability of the VC compounds could be predicted from cohesive energies, formation enthalpies, and C vacancy in the crystal structure. The more negative the formation enthalpies of the VC compounds, the more stable the compound. Also, the C vacancy in the crystal structure of VC decreased the compound's stability. The formation energies calculated in this study were −0.541, −0.522, −0.466, −0.405 and –0.324 for V_6C_5, V_8C_7, V_2C, VC, V_4C_3 respectively. Therefore, the order of decreasing stability for the carbides was determined to be, $V_6C_5 > V_8C_7 > V_2C > VC > V_4C_3$ [91]. These findings indicate that V_6C_5 is the least reactive in the environment and retains its useful properties better than the other binary compounds. This result was also confirmed by Wang *et al* and Sun *et al* [85, 92]. As illustrated previously (figure 6(b)), the density of states (DOS) structure of VC, V_4C_3, and V_8C_7 all have similar DOS structures with electronic core structures due to the C2p and V3d in −16 and −8 eV [85]. However, many atoms in the V_8C_7 unit cell resulted in higher DOS values. Also, all VC are considered metallic compounds because of their finite TDOS at the Fermi level [91]. The bonding between the metal (d) and non-metal (p) electrons results in

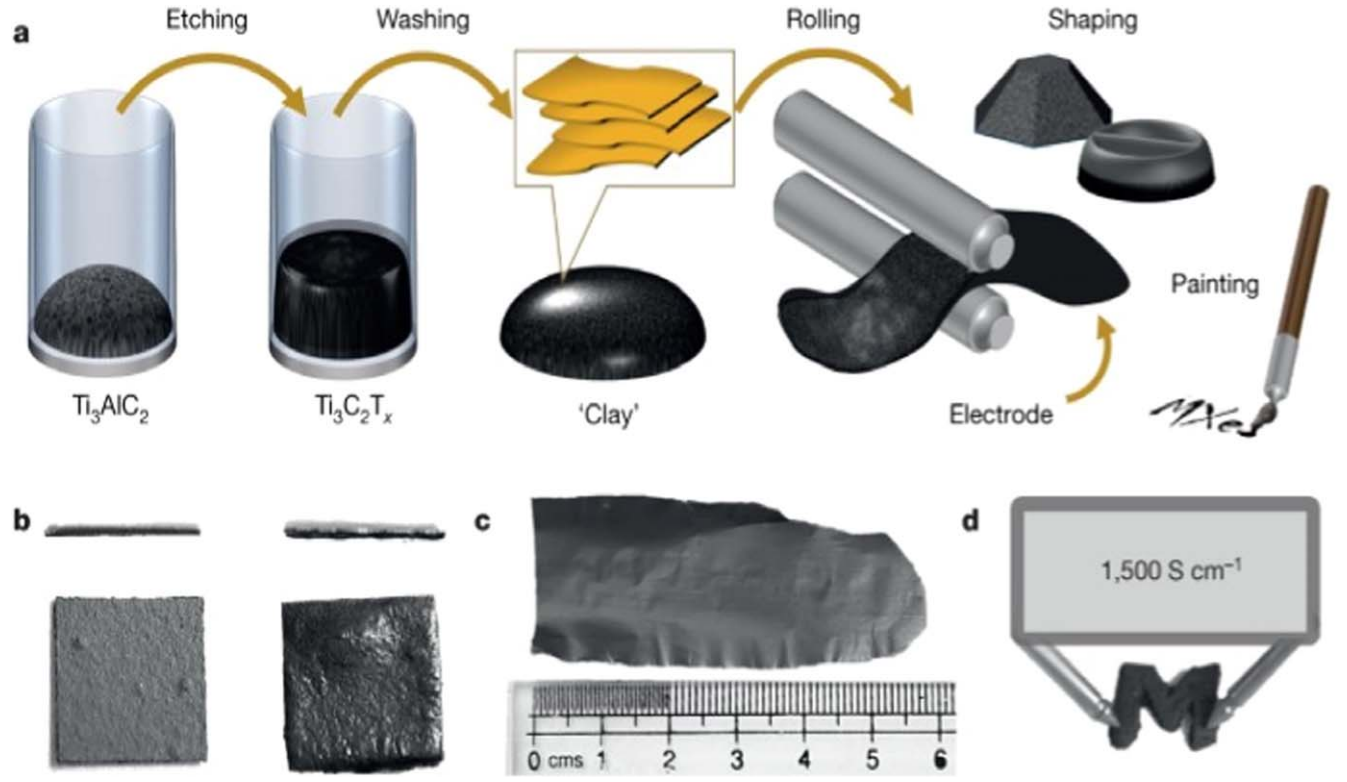

Figure 7. Clay-like structure of MXenes. Reproduced from [70], with permission from Springer Nature.

shear-resistive covalent bonding, which gives the VC compound its hardness [93].

3.3. Effect of interlayer spacing and functionalization of vanadium carbide MXenes in energy storage devices

2D layered materials generally can host cations of different sizes. This phenomenon is described as intercalation, the alterable exsiccation or embedding of a molecule or ion into the interlayers of layered structures [3, 94]. The intercalation mechanism became popular through first-generation lithium-ion batteries (LIBs). It is essential to note that the etching method determines the interlayer spacing [95]. Wu *et al* reported that etching with fluoride salt (NaF) and HCl and HF yields a *c* lattice parameter (*c*-LP) of 22.0 Å and 19.8 Å respectively. [33]. Furthermore, the distance between MXene layers is closely linked to the number of intercalated water molecules. MXenes etched with HCl, and LiF (cations and water intercalated) are about 2.8 Å larger than the 50% HF-etched MXene because of a layer of water and cations between the MXene layers in the previous case [96]. Controlling the interlayer spacing of MXenes and maximizing its use in energy storage applications, purification, and biomedical engineering can be achieved through cation intercalation. Understanding the intercalation's structural effects helps discover the best conditions for intercalating large cations, as large cations generally decrease the specific capacitance because of a void created in the electrode. Therefore, there is a trade-off between larger interlayer spacing and increased capacitance depending on the application of the MXene [3].

In a bid to improve the interlayer spacing and electrochemical performance of V_2C MXene by Liu *et al*, the MXene was first lithiated, which improved the peaks from $2\theta = 8.14°$ to $2\theta = 8.03°$. When tested, the prelithiated MXene demonstrated a higher specific capacity and reduced Li^+ ions during SEI formation. Figure 8(a) shows the schematic of the working conditions of the MXenes before and after prelithiation, demonstrating that prelithiation can increase the MXene interlayers and recompense the Li loss in the initial cycle leading to a high reversible capacity [97]. Another study by Naguib *et al* revealed that upon mixing of V_2CT_x with -TBAOH for two hours, a peak shift from 2θ of 8.9° to 4.6° (*c*-LP from 19.9 Å to 38.6 Å) was observed. The total space increase was ~9.4 Å. Also, treatment of V_2CT_x with 50% aqueous choline hydroxide and n-butylamine resulted in *c*-LP of 36.0 Å and 36.3 Å [67]. To achieve a high-capacity rechargeable aluminum electrode, the V_2CT_x was also treated with TBAOH, which led to a 5.73 Å increase in the *c*-LP and was delaminated with NMP, a famous intercalation material for 2D structures. Figure 8(b) shows the XRD patterns of V_2CT_x treated with TBAOH and V_2CT_x without treatment which shows a 5.73 Å increase in the interlayer spacing and, ultimately, an increase in the specific capacity [59]. Another material intercalated with V_2CT_x was Sn. Herein, V_2CT_x was immersed in 2 M KOH at 40°C for 1 d and then transferred to 0.2 M stannic chloride at 40°C for 2 more days. V_2C@Sn was obtained after washing and freeze-drying. The XRD results show an enlarged *c*-LP of about 19 Å, indicating increased interlayer spacing using Sn as an intercalant. This expanded interlayer led to the synthesis of a material producing a

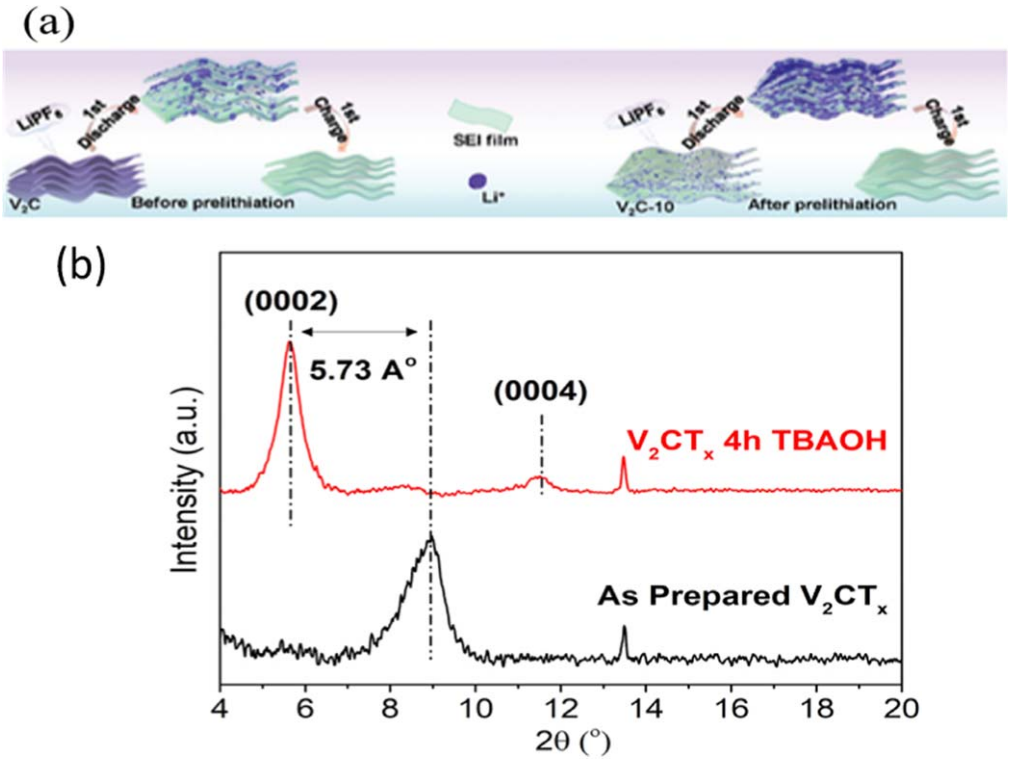

Figure 8. (a) Schematic of the working conditions of the MXenes before and after prelithiation Adapted from [97] with permission from WILEY-VCH, copyright 2020. (b): XRD Patterns of V_2CT_x Treated with TBAOH And V_2CT_x Without Treatment Reprinted (adapted) with permission from [59]. Copyright (2017) American Chemical Society.

coulombic efficiency of 96% and a high discharge capacity of 941 mAh g^{-1} at 0.3 A g^{-1} current density [98]. Also, Sn's valence change being reversible contributed to the LIB capacity and stability.

4. Vanadium carbide MXene application in energy storage devices

The emission of greenhouse gases and the strive to save the planet have led many companies to invest in developing more sustainable energy sources, thereby reducing the heavy dependence on fossil fuels [99, 100]. Renewable energy sources such as wind, solar and tidal energy offer an attractive alternative to fossil fuel because they reduce environmental pollution, improve economic development by providing job opportunities, and lower electricity costs, especially in rural, underdeveloped areas [101, 102]. However, energy generation from these sources is limited by weather inconsistencies and climate changes resulting in erratic power production. Therefore, energy storage devices are essential for storing and harvesting energy from different natural resources and conversion into electrical energy for on-demand use [103]. MXene-based materials for energy storage devices are integral in integrating high power, high energy, and long-term features into renewable energy devices [103]. Generally, MXenes with low formula weights, like Ti_2C, Nb_2C, V_2C, and Sc_2C, have demonstrated better gravimetric capacities than their higher-weight counterparts [103]. To this end, M_2X electrodes are expected to demonstrate better gravimetric capacities than M_3X_2 and M_4X_3 [104]. The current order of MXenes specific capacity is $Ti_2C < Nb_2C < V_2C$, indicating that vanadium carbide MXenes have the highest specific capacity[47]. This correlates with previous research, which estimated the theoretical capacity of V_2C as 940 mAh g^{-1} [105]. Materials with high specific capacity allow for energy storage devices with improved storage capacity to be synthesized. The high specific capacity of vanadium-based MXenes was illustrated by Zhou *et al*, where V_4C_3 was used as the anode material that could provide a high specific capacity of 225 mAh g^{-1} after 300 charge–discharge cycles [54].

4.1. Vanadium carbide MXenes in batteries

4.1.1. Vanadium carbide MXenes in Li-ion batteries. The development and application of LIBs in electric vehicles and portable electronics have reduced the dependence on fossil fuels due to the large energy density of LIBs [106]. It is no surprise that MXenes have entered the race as a formidable competitor because it improves LIBs and promises successful growth into batteries other than Li-based batteries [107]. The performance of Li batteries can be enhanced using MXene with different functionalization, formula weight, and type. The functionalization of MXenes affects its overall character, where research has shown that non-functionalized MXene displays magnetic properties while functionalized MXenes are semi-conductive [107]. In general, the surface

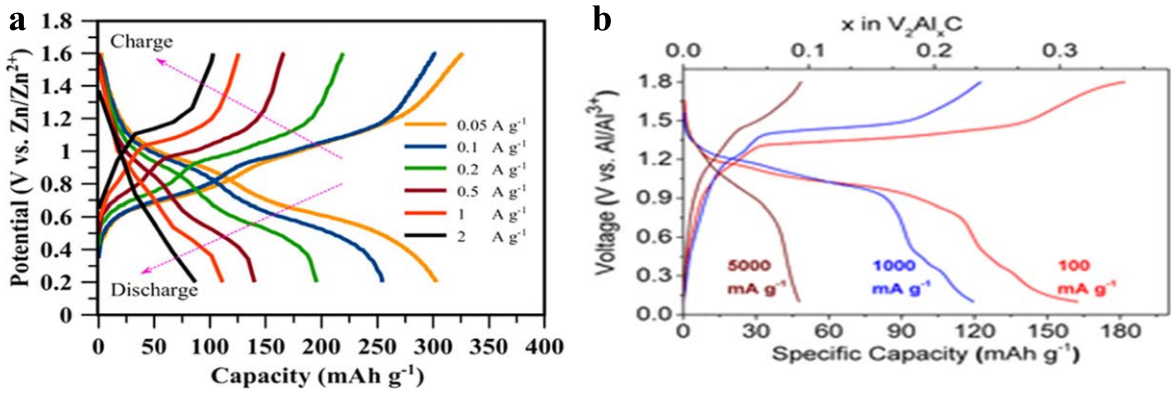

Figure 9. (a) Charge–discharge profiles of $V_2O_x@V_2CT_x$ from 0.05 and 2 A g^{-1}. Reprinted (adapted) with permission from [111]. Copyright (2020) American Chemical Society. [111] (b) charge–discharge profiles of the FL-V_2CT_x at different current densities in aluminum batteries. Reprinted (adapted) with permission from [59]. Copyright (2017) American Chemical Society.

terminations determine the performance of the MXenes with bare MXene. Oxygen terminations have higher capacity and excellent Li-ion transport instead of the hydroxyl and fluorine terminations, resulting in lower capacity and hindering Li-ion transport [47]. If the terminations are non-native, like Cl, an increase in the interlayer spacing occurs, and also, the adverse effects of the native OH and F functional groups are alleviated [107]. Functionalization also increases the interlayer spacing, thereby increasing Li uptake and transport. This is particularly important when using large ions of organic electrolyte (0.65–1.3 nm). These impede transportation between the MXene layers and limit the specific capacitance and rate capability [108]. This phenomenon was proven by Wang *et al* which dmonstrated that functionalizing vanadium carbide MXenes with atomic Sn^{4+} improves the Lithium-ion battery (LIB) battery performance and provides a reasonable rate and cycling stability [98]. This result was achieved by increasing the interlayer spacing of the MXene and the formation of the V–O–Sn bonds. An almost 100% reversible lithium storage capacity of 1262.9 mAh g^{-1} was achieved after 90 cycles when the current density was 0.1 A g^{-1}. Comparing this result with Mashtalir *et al* shows a reduced capacity of 410 mAh g^{-1} at a 1C cycling rate. This shows that to achieve the full MXene's full potential; an increased interlayer spacing is essential as it facilitates easy ion intercalation and storage, increasing the amount of energy a battery can store. Furthermore, studies by Yan *et al* illustrate that upon the decoration of V_2C with oxygen/sulfur, the resulting MXenes, after lithiation, remain metallic, lower the Li diffusion barrier, and increase their Li capacity, which validates their great potential alternative anodes [109].

4.1.2. Vanadium carbide MXenes in Non-Li batteries. There is no question that the massive development in the use of lithium-based energy storage devices might strain the world's lithium supply in the future. Hence, new chemistries of non-LIBs like Mg-ion, Al-ion, Na-ion, K-ion, and Ca-ion batteries have arisen as suitable substitutes in the next phase of sustainable energy technologies [84, 88–90]. As in Li-based batteries, vanadium-based MXenes promote the enhanced performance of non-Li batteries offering increased interlayer spacing, which translates into better storage capacity. V_2CT_x demonstrated good cycling stability and high-rate capability when used as an anode in Na-ion batteries.

A study on charge storage mechanisms confirmed that the redox reaction at the transition metal (M) site in MXene is responsible for electrochemical storage [56]. Wei *et al* confirmed the high-rate capacity of V_2CT_x MXene intercalated with Mn^{2+} and tested in a sodium-ion battery was 425 mAh g^{-1} at a current density of 0.005 A g^{-1}. This was due to the increased interlayer spacing provided by the intercalation of the Mn^{2+} [110]. It was also discovered that the Na^+ storing capacity in $V_2C@Mn$ is mainly capacitive with a linear relationship with current density and capacity [110]. Vanadium MXenes have also proven to be brilliant cathode materials in aqueous zinc-ion batteries, as shown by Venkatkarthick *et al.* Here, V_2CT_x, electrodes had enhanced capacities of 304 and 84 mA g^{-1} at current densities ranging from 0.05 and 2 A g^{-1}, respectively [111]. The improved permeability, lower interfacial resistance for the electrolyte, good conductivity, and high surface areas correlate to V_2C high specific capacity [103, 112]. Figure 9(a) shows the charge–discharge profiles of $V_2O_x@V_2CT_x$. The figure shows that even at high current densities of 1 and 2 A g^{-1}, noticeable charge/discharge plateaus are noticed [111].

In aluminum batteries, V_2CT_x has proven to be an excellent cathode material even with the high charge density of Al^{3+} cations and its strong interactions with the host lattice [113, 114]. Vahid Mohammadi *et al*, V_2CT_x achieved specific capacities of 300 mAh g^{-1} at high discharge rates and discharge potentials. The V_2CT_x MXenes were pre-intercalated with TBAOH and then delaminated into single sheets, improving the batteries' interlayer spacing and, ultimately, specific capacity [59]. Figure 9(b) shows the charge–discharge profiles of V_2C in aluminum batteries. From the diagram, the electrodes displayed a high-rate capability. It also indicates that after charging at very high rates (1000 mA g^{-1}) and discharging at slower rates (100 mA g^{-1}) after 100 cycles, the cathode (intercalated MXene) could still produce a good

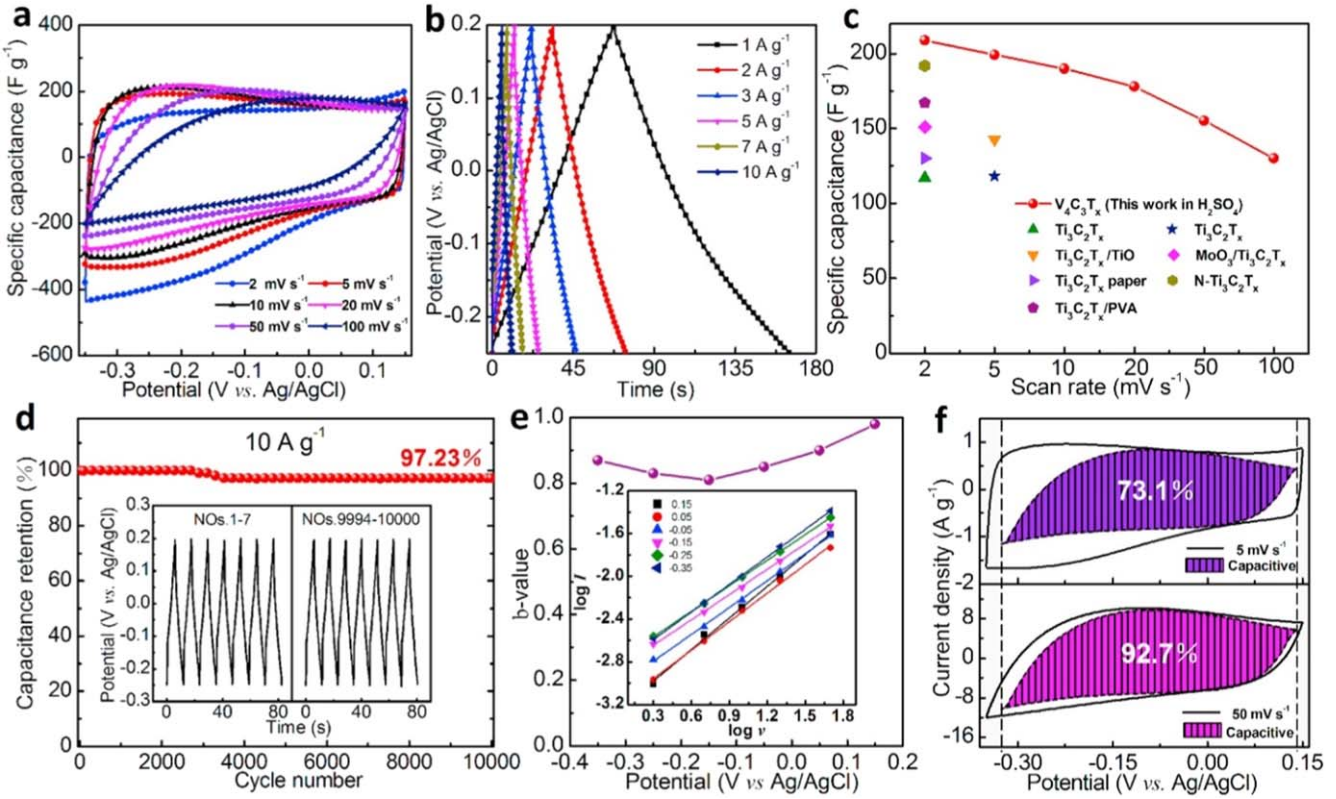

Figure 10. $V_4C_3T_x$ electrodes electrochemical performance in a 1 M H_2SO_4 electrolyte. (a) $V_4C_3T_x$ electrode CV curves at various scan rates. (b) The $V_4C_3T_x$ electrode's galvanostatic charge–discharge curves at various current densities ranging from 1 to 10 A g^{-1}. (c) The electrodes' gravimetric specific capacitance displayed as a function of scan rate. (d) The $V_4C_3T_x$ electrode's cycling performance at 10 A g^{-1}, with galvanostatic cycling data insets. (e) $V_4C_3T_x$ electrode *b*-values; inset plots log I versus log v (f) Capacitive contribution to total current at chosen scan rates as determined by CV partition analysis. Reprinted from [51] Copyright (2019), with permission from Elsevier.

discharge capacity of 76 mAh g^{-1} and columbic efficiency of approximately 96.6% [59].

4.2. Vanadium carbide MXenes in supercapacitors

Supercapacitors have high power densities, longer operating life, more significant power, and high-power rates. Supercapacitors can also be included within a battery to improve the size while improving its power requirements and increasing the lifetime [1, 115]. The breakthrough for supercapacitors has been restricted due to the lack of cheap, stable, and highly efficient electrode materials with good conductivity. Some of the issues with the researched electrode materials include insufficient interlayer spacing, poor conductivity, and volume expansion [21, 116, 117]. MXenes, on the other hand, have proven to have larger interlayer spacing, quick ion diffusion, controllable structure and morphology, high surface area, and good electrical conductivity, which is a crucial factor in supercapacitors [1]. Wang *et al* study of vanadium carbide MXenes again illustrated high capacitance and retention rate when tested as supercapacitor electrodes. The research discovered that $V_4C_3T_x$ shows a high capacitance of 209 F g^{-1} at 2 mV s^{-1}, good rate performance, and stable long cyclic performance with capacitance retention rate 97.23% after 10 000 cycles at 10 A g^{-1} in 1 M H_2SO_4. This was due to the wide interlayer spacing, large specific surface area, good pore volumes, and excellent hydrophilicity [51].

Figure 10 shows the electrochemical performance of $V_4C_3T_x$ electrodes [51]. The cyclic voltammetry curves in figure 10(a) show that the charge and discharge capacitance differ between the given potential window. This is due to the irreversibly intercalated cations trapped during the discharge process between the $V_4C_3T_x$ layers [49]. Figure 10(b) shows GCD curves and cyclic performance at various current density between −0.25V and 0.2V (versus Ag/AgCl). The shapes obtained from the CV and GCD tests show that the $V_4C_3T_x$ electrodes exhibit typical capacitive behavior. Figure 10(c) proves that $V_4C_3T_x$ has a higher specific capacitance than previously reported Ti-based MXenes with a specific capacitance of 209 F g^{-1}. This result is proven in previous reports where Ti-based MXenes had a capacitance of 143 F g^{-1} [118], 117 F g^{-1}[119], 118 F g^{-1} [120], and 192 F g^{-1}[121]. It confirms the inverse relationship between scan rate and capacitance [51]. As the gravimetric specific capacitance of the electrode decreases, there is an increase in the scan rate due to limited kinetics [51]. At gravimetric capacitance of 209, 199, 190, 178, 155, and 130 F g^{-1} , the scan rates were 2, 5, 10, 20 , 50, and 100 mV s^{-1}, respectively [51]. From figure 10(d), the capacitance retention is 97.23% even after 10 000 cycles at 10 A g^{-1} proving excellent capacitive behaviors. Figure 10(f) shows that scan speeds

Table 2. Capacitance of vanadium MXenes in energy storage devices.

Battery composition	Capacitance (mAh g^{-1})	Supercapacitor composition	Capacitance (F g^{-1})	References
Sn^{4+} functionalized V_2CT_x in Li-ion batteries	1262.9	Bare $V_4C_3T_x$	209	[51, 98]
Bare V_2CT_x in Li-ion batteries	410	Bare V_2CT_x	487	[49, 109]
Mn^{2+} functionalized V_2CT_x in Na-ion batteries	425	Bare $V_4C_3T_x$	330	[110, 123]
Bare V_2CT_x in Al-ion batteries	300	Bare V_2CT_x	181.1	[59, 124]
Bare V_2CT_x in Al-ion batteries		Bare $V_8C_7T_x$	161.7	[125]

below 50 mV s^{-1} have little or no effect on the overall capacitance, demonstrating that redox processes are not diffusion-limited but classified as semi-diffusion-controlled processes [122]. Dall'Agnese *et al*, V_2CT_x was used as a cathode material in a sodium ion capacitor. An entire asymmetric cell was assembled using hard carbon as an anode material in their work. The cell achieved the capacity of 50 mAh g^{-1} with a maximum cell voltage of 3.5 V. The results proved that V_2CT_x could be an attractive cathode material with a wide operating window.

Shan *et al* reported the electrochemical behavior of V_2C in three aqueous electrolytes: $MgSO_4$, H_2SO_4, and KOH. Exceptional specific capacitances were achieved, specifically 487 F g^{-1} in 1 M H_2SO_4, 225 F g^{-1} in 1 M $MgSO_4$, and 184 F g^{-1} in 1 M KOH. This work shows V_2C MXene as a promising electrode for energy storage using aqueous electrolytes [49]. Vanadium carbide (V_4C_3) MXenes were successfully synthesized by Syamsai *et al* through HF etching. Testing the electrochemical performance revealed the specific capacitance to be 330 F g^{-1} at 5 mV s^{-1} in 1 M H_2SO_4 electrolyte and a high retention rate of 90% even after 3000 cycles [123]. This result signifies the stability of V_4C_3 as an electrode and a decline in the charge storage capacity of 10% after charging and discharging 3000 times. Hongtian *et al* demonstrated the versatility of V_2CT_x as a supercapacitor electrode using seawater as the electrolyte. A capacitance of 181.1 F g^{-1}, volumetric specific capacitance of 317.8 F cm^{-3}, and an 89.1% capacitance retention after 5000 cycles were achieved[124]. A polycrystalline intermetallic vanadium carbide (V_8C_7) was effectively synthesized and tested as an electrode material for electrochemical capacitors by Zhang *et al.* The V_8C_7 electrode was tested in 1.0 M Na_2SO_4 at a specific current density of 1 A g^{-1} and had a large specific capacitance of 161.7 F g^{-1}. The electrode retained 92.8% of the specific capacitance after 10 000 cycles. 83.3% of the initial capacitance was maintained even at a high current density of 10 A g^{-1} [125]. The large ionic radius of potassium makes it difficult for K^+ ion capacitors to expand, even though the low cost of these materials makes it advantageous [117]. The results from this study indicated that materials with small interlayer spacing and open framework are unpromising for use in electrodes and would produce low capacitance. However, Ming *et al* tested V_2CT_x as a supercapacitor electrode. The device achieved a high energy density of 145 Wh kg^{-1} at a power density of 112.6 W kg^{-1}, suggesting that K–V_2C can be promising electrodes in mobile ion capacitors [126].

To summarize, table 2 below shows a summary of vanadium Mxenes used as electrodes in supercapacitors and batteries.

5. Gaps in the current knowledge

Since the discovery of the first MXene, many questions are still left unanswered to maximize the capacity of MXenes fully. More than a hundred different MAX phase compositions have been predicted and studied, leaving a plethora of ternary carbides to be converted into MXenes. Any layered transition metal carbide or nitride with the formula $M_{n+1}X_n$ layers and separated with A-group metals can be etched into a MXene. Therefore, the synthesis of MXenes is a significant research direction. The HF synthesis method with the highest yield is LiF-HCl etching, which yields 91.3% [57]. However, other non-toxic methods like halogen etching of the vanadium MXenes should be implemented. In energy-storage applications, more work is required to minimize the first-cycle irreversibility and capacity drop observed after Li- and Na-ion intercalation. Also, an in-depth understanding of the intercalation mechanism of multivalent and large organic ions would deliver essential strategies for emerging electrode materials for the next group of batteries and supercapacitors. Finally, another critical research path is the in-depth research on aligning the theoretical capacity of vanadium carbide MXenes with the practical, specific capacity. V_2C has a theoretically higher specific capacity in LIBs than all other MXenes. A deep understanding of the electrochemical energy storage mechanisms of MXenes, the pure synthesis procedure for vanadium MXenes, and the influence of the surface terminations would help to develop more useful electrodes.

Furthermore, using MXenes as flexible and transparent electrodes is extremely important for the next generation of consumer electronics. Also, the scale-up of MXene synthesis is crucial to take MXenes from the laboratory to the industry. Shuck *et al* developed a model that mitigates the safety concerns during MXene synthesis and increases the yield of the MXenes [127]. However, an in-depth understanding of the synthesis-structure-property relationship is required to scale-up MXene production. Lastly, there has been much research on titanium-based MXenes, but only a few on their vanadium counterparts. Hence more attempts at utilizing V_2C as a promising electrode should be investigated in both batteries and supercapacitors.

6. Conclusion

Developing improved electrode materials can meet the high need for electrochemical energy storage systems. The disadvantages of various electrode materials, such as carbon and its derivatives, metal oxides, and conducting polymers, have sparked interest in recent decades; therefore, new electrode materials are being investigated. This has led to the discovery of new 2D materials with separate layers in 2D. In 2011, a new 2D electrode material called MXene was studied. MXenes also have outstanding qualities such as brittleness, high melting point, oxidation resistance, high electrical and thermal conductivity, hydrophilic nature, compositional diversity, a wide surface area region, and a proclivity to support a wide range of intercalants. As a result, it was created as an alternative to the materials used in prior electrodes. The vanadium MXene, in particular, has a high theoretical capacity of about 940mAg^{-1}, making it a good candidate for synthesizing high-capacity energy storage devices. In this study, recent technologies for synthesizing 2D MXenes and their applications are discussed in this review with specificity in vanadium carbide MXenes.

However, the pure synthesis of V_2C is still an issue due to the low formation energy of V_2C in addition to the toxicity of the hydrofluoric acid synthesis process discussed. It can also be seen that V_2C has good excellent metallic conductivity; however, the fabrication of high energy density electrode materials is still pending to provide for the popularity of wearable and flexible devices. Also, storing these V_2C MXenes is a big issue due to the multivalent state of vanadium. However, it is advised that storage should be done in an oxygen-free low-temperature environment or dissolved in a polar solvent to reduce the degradation of the MXene. Lastly, the benefits of using vanadium MXene hybrids in improving the restacking issue MXenes face and the electronic conductivity, stability, and easy ion/electron transport is discussed. To this end, MXenes provide a promising starting point for future research into energy storage applications.

Data availability statement

All data that support the findings of this study are included within the article (and any supplementary files).

ORCID iDs

Ayomide Adeola Sijuade https://orcid.org/0000-0002-0147-019X
Vincent Obiozo Eze https://orcid.org/0000-0003-1484-2922
Okenwa I Okoli https://orcid.org/0000-0003-1918-6442

References

[1] Chu S and Majumdar A 2012 Opportunities and challenges for a sustainable energy future *Nature* **488** 294–303
[2] Garg R, Agarwal A and Agarwal M 2020 A review on MXene for energy storage application: effect of interlayer distance *Mater. Res. Express* **7** 022001
[3] Chaudhari N K, Jin H, Kim B, San Baek D, Joo S H and Lee K 2017 MXene: an emerging two-dimensional material for future energy conversion and storage applications *J. Mater. Chem.* A **5** 24564–79
[4] Reddy A L M, Gowda S R, Shaijumon M M and Ajayan P M 2012 Hybrid nanostructures for energy storage applications *Adv. Mater.* **24** 5045–64
[5] Dunn B, Kamath H and Tarascon J-M 2011 Electrical energy storage for the grid: a battery of choices *Science* **334** 928–35
[6] Shah Z M and Khanday F A 2021 Analysis of disordered dynamics in polymer nanocomposite dielectrics for the realization of fractional-order capacitor *IEEE Trans. Dielectr. Electr. Insul.* **28** 266–73
[7] Frackowiak E 2007 Carbon materials for supercapacitor application *Phys. Chem. Chem. Phys.* **9** 1774–85
[8] Danilovic N *et al* 2014 Using surface segregation to design stable Ru-Ir oxides for the oxygen evolution reaction in acidic environments *Angew. Chem. Int. Ed.* **53** 14016–21
[9] Yang L *et al* 2013 Tuning the catalytic activity of Ru@Pt core–shell nanoparticles for the oxygen reduction reaction by varying the shell thickness *J. Phys. Chem.* C **117** 1748–53
[10] Zheng H-B *et al* 2018 Tuning the catalytic activity of Ir@Pt nanoparticles through controlling Ir core size on cathode performance for PEM fuel cell application *Front. Chem.* **6** 299
[11] Oh A *et al* 2016 Rational design of Pt–Ni–Co ternary alloy nanoframe crystals as highly efficient catalysts toward the alkaline hydrogen evolution reaction *Nanoscale* **8** 16379–86
[12] Yoon J *et al* 2016 Synthesis of bare Pt3Ni nanorods from PtNi@Ni core–shell nanorods by acid etching: one-step surfactant removal and phase conversion for optimal electrochemical performance toward oxygen reduction reaction *CrystEngComm* **18** 6002–7
[13] Bruce P G, Scrosati B and Tarascon J-M 2008 Nanomaterials for rechargeable lithium batteries *Angew. Chem. Int. Ed.* **47** 2930–46
[14] Yang Y, Zheng G, Misra S, Nelson J, Toney M F and Cui Y 2012 High-capacity micrometer-sized Li2S particles as cathode materials for advanced rechargeable lithium-ion batteries *J. Am. Chem. Soc.* **134** 15387–94
[15] Rolison D R and Nazar L F 2011 Electrochemical energy storage to power the 21st century *MRS Bull.* **36** 486–93
[16] Fu L J *et al* 2006 Surface modifications of electrode materials for lithium ion batteries *Solid State Sci.* **8** 113–28
[17] Liu C, Li F, Ma L-P and Cheng H-M 2010 Advanced materials for energy storage *Adv. Mater.* **22** E28–62
[18] Fang T Improving the electrochemical performance of LiCoO2 cathode by nanocrystalline ZnO coating, Accessed: Nov. 07, 2021. [Online]. Available: https://core.ac.uk/reader/61706580
[19] Pandolfo A G and Hollenkamp A F 2006 Carbon properties and their role in supercapacitors *J. Power Sources* **157** 11–27
[20] De B, Banerjee S, Verma K D, Pal T, Manna P K and Kar K K 2020 Carbon nanotube as electrode materials for supercapacitors *Handbook of Nanocomposite Supercapacitor Materials II: Performance* ed K K Kar (Cham: Springer International Publishing) 229–43
[21] Sahoo N G, Pan Y, Li L and Chan S H 2012 Graphene-based materials for energy conversion *Adv. Mater.* **24** 4203–10
[22] Knoll C *et al* 2019 Magnesium oxide from natural magnesite samples as thermochemical energy storage material *Energy Procedia* **158** 4861–9
[23] Sevilla M and Mokaya R 2014 Energy storage applications of activated carbons: supercapacitors and hydrogen storage *Energy Environ. Sci.* **7** 1250–80

[24] Majumdar D 2018 An overview on ruthenium oxide composites—challenging material for energy storage applications *Mater. Sci. Res. India* **15** 30–40

[25] Liu T 2020 Overlooking issues and prospective resolutions behind the prosperity of three-dimensional porous carbon supercapacitor electrodes *Front. Energy Res.* **8** 125

[26] Hillier N, Yong S and Beeby S 2020 The good, the bad and the porous: a review of carbonaceous materials for flexible supercapacitor applications *Energy Rep.* **6** 148–56

[27] Gamby J, Taberna P L, Simon P, Fauvarque J F and Chesneau M 2001 Studies and characterisations of various activated carbons used for carbon/carbon supercapacitors *J. Power Sources* **101** 109–16

[28] Zhang Y, Yang S, Wang S, Liu X and Li L 2019 Microwave/freeze casting assisted fabrication of carbon frameworks derived from embedded upholder in tremella for superior performance supercapacitors *Energy Storage Mater.* **18** 447–55

[29] Han Z J, Pineda S, Murdock A T, Seo D H, (Ken) Ostrikov K and Bendavid A 2017 RuO2-coated vertical graphene hybrid electrodes for high-performance solid-state supercapacitors *J. Mater. Chem.* A **5** 17293–301

[30] Lv P, Tang X, Zheng R, Ma X, Yu K and Wei W 2017 Graphene/polyaniline aerogel with superelasticity and high capacitance as highly compression-tolerant supercapacitor electrode *Nanoscale Res. Lett.* **12** 630

[31] Naguib M *et al* 2011 Two-dimensional nanocrystals produced by exfoliation of Ti3AlC2 *Adv. Mater.* **23** 4248–53

[32] Gao L *et al* 2020 MXene/polymer membranes: synthesis, properties, and emerging applications *Chem. Mater.* **32** 1703–47

[33] Wu M, Wang B, Hu Q, Wang L and Zhou A 2018 The synthesis process and thermal stability of V_2C MXene *Materials* **11** 11

[34] Fu L and Xia W 2021 MAX phases as nanolaminate materials: chemical composition, microstructure, synthesis, properties, and applications *Adv. Eng. Mater.* **23** 2001191

[35] Sharma G, Naguib M, Feng D, Gogotsi Y and Navrotsky A 2016 Calorimetric determination of thermodynamic stability of MAX and MXene phases *J. Phys. Chem.* C **120** 28131–7

[36] Mishra A, Srivastava P, Mizuseki H, Lee K-R and Singh A K 2016 Isolation of pristine MXene from Nb_4AlC_3 MAX phase: a first-principles study *Phys. Chem. Chem. Phys.* **18** 11073–80

[37] Berdiyorov G R 2016 Optical properties of functionalized Ti3C2T2 (T = F, O, OH) MXene: first-principles calculations *AIP Adv.* **6** 055105

[38] Naguib M, Mochalin V N, Barsoum M W and Gogotsi Y 2014 25th anniversary article: MXenes: a new family of two-dimensional materials *Adv. Mater.* **26** 992–1005

[39] Rajan A C *et al* 2018 Machine-learning-assisted accurate band gap predictions of functionalized MXene *Chem. Mater.* **30** 4031–8

[40] Hantanasirisakul K and Gogotsi Y 2018 Electronic and optical properties of 2D transition metal carbides and nitrides (MXenes) *Adv. Mater.* **30** 1804779

[41] Naguib M *et al* 2013 New two-dimensional niobium and vanadium carbides as promising materials for Li-Ion batteries *J. Am. Chem. Soc.* **135** 15966–9

[42] Hu Q *et al* 2013 MXene: a new family of promising hydrogen storage medium *J. Phys. Chem.* A **117** 14253–60

[43] Lee E, VahidMohammadi A, Yoon Y S, Beidaghi M and Kim D-J 2019 Two-dimensional vanadium carbide MXene for gas sensors with ultrahigh sensitivity toward nonpolar gases *ACS Sens.* **4** 1603–11

[44] Wang L *et al* 2016 Loading actinides in multilayered structures for nuclear waste treatment: the first case study of uranium capture with vanadium carbide MXene *ACS Appl. Mater. Interfaces* **8** 16396–403

[45] Xin M, Li J, Ma Z, Pan L and Shi Y 2020 MXenes and their applications in wearable sensors *Front. Chem.* **8** 297

[46] Zhang Y-Z *et al* 2020 MXene hydrogels: fundamentals and applications *Chem. Soc. Rev.* **49** 7229–51

[47] Xie Y *et al* 2014 Role of surface structure on Li-ion energy storage capacity of two-dimensional transition-metal carbides *J. Am. Chem. Soc.* **136** 6385–94

[48] Khazaei M, Mishra A, Venkataramanan N S, Singh A K and Yunoki S 2019 Recent advances in MXenes: from fundamentals to applications *Curr. Opin. Solid State Mater. Sci.* **23** 164–78

[49] Shan Q *et al* 2018 Two-dimensional vanadium carbide (V_2C) MXene as electrode for supercapacitors with aqueous electrolytes *Electrochem. Commun.* **96** 103–7

[50] VahidMohammadi A, Mojtabavi M, Caffrey N M, Wanunu M and Beidaghi M 2019 Assembling 2D MXenes into highly stable pseudocapacitive electrodes with high power and energy densities *Adv. Mater.* **31** 1806931

[51] Wang X *et al* 2019 Two-dimensional V4C3 MXene as high performance electrode materials for supercapacitors *Electrochim. Acta* **307** 414–21

[52] Tran M H *et al* 2018 Adding a new member to the MXene family: synthesis, structure, and electrocatalytic activity for the hydrogen evolution reaction of $V_4C_3T_x$ *ACS Appl. Energy Mater.* **1** 3908–14

[53] Anasori B, Lukatskaya M R and Gogotsi Y 2017 2D metal carbides and nitrides (MXenes) for energy storage *Nat. Rev. Mater.* **2** 16098

[54] Zhou J *et al* 2019 Synthesis and lithium ion storage performance of two-dimensional V4C3 MXene *Chem. Eng. J.* **373** 203–12

[55] Lei J-C, Zhang X and Zhou Z 2015 Recent advances in MXene: preparation, properties, and applications *Front. Phys.* **10** 276–86

[56] Bak S-M *et al* 2017 Na-Ion intercalation and charge storage mechanism in 2D vanadium carbide *Adv. Energy Mater.* **7** 1700959

[57] Guan Y *et al* 2020 A hydrofluoric acid-free synthesis of 2D vanadium carbide (V2C) MXene for supercapacitor electrodes *2D Mater.* **7** 025010

[58] Pang S-Y *et al* 2019 universal strategy for HF-free facile and rapid synthesis of two-dimensional MXenes as multifunctional energy materials *J. Am. Chem. Soc.* **141** 9610–6

[59] VahidMohammadi A, Hadjikhani A, Shahbazmohamadi S and Beidaghi M 2017 Two-dimensional vanadium carbide (MXene) as a high-capacity cathode material for rechargeable aluminum batteries *ACS Nano* **11** 11135–44

[60] Yoon Y *et al* 2019 Precious-metal-free electrocatalysts for activation of hydrogen evolution with nonmetallic electron donor: chemical composition controllable phosphorous doped vanadium carbide MXene *Adv. Funct. Mater.* **29** 1903443

[61] Bhat A, Anwer S, Bhat K S, Mohideen M I H, Liao K and Qurashi A 2021 Prospects challenges and stability of 2D MXenes for clean energy conversion and storage applications *Npj 2D Mater. Appl.* **5** 1–21

[62] Cambaz G Z, Yushin G N, Gogotsi Y and Lutsenko V G 2006 Anisotropic etching of SiC whiskers *Nano Lett.* **6** 548–51

[63] Liu F *et al* 2017 Preparation of high-purity V2C MXene and electrochemical properties as Li-Ion batteries *J. Electrochem. Soc.* **164** A709

[64] Li M *et al* 2019 Element replacement approach by reaction with lewis acidic molten salts to synthesize nanolaminated MAX phases and MXenes *J. Am. Chem. Soc.* **141** 4730–7

[65] Zhou C *et al* 2022 A review of etching methods of MXene and applications of MXene conductive hydrogels *Eur. Polym. J.* **167** 111063

[66] Feng A *et al* 2017 Fabrication and thermal stability of NH4HF2-etched Ti3C2 MXene *Ceram. Int.* **43** 6322–8

[67] Naguib M, Unocic R R, Armstrong B L and Nanda J 2015 'Large-scale delamination of multi-layers transition metal carbides and carbonitrides 'MXenes *Dalton Trans.* **44** 9353–8

[68] Zada S *et al* 2020 Algae extraction controllable delamination of vanadium carbide nanosheets with enhanced near-infrared photothermal performance *Angew. Chem. Int. Ed.* **59** 6601–6

[69] Zhu K *et al* 2019 Synthesis of Ti2CTx MXene as electrode materials for symmetric supercapacitor with capable volumetric capacitance *J. Energy Chem.* **31** 11–8

[70] Ghidiu M, Lukatskaya M R, Zhao M-Q, Gogotsi Y and Barsoum M W 2014 Conductive two-dimensional titanium carbide 'clay' with high volumetric capacitance *Nature* **516** 7529

[71] Liu F *et al* 2017 Preparation of Ti3C2 and Ti2C MXenes by fluoride salts etching and methane adsorptive properties *Appl. Surf. Sci.* **416** 781–9

[72] Soundiraraju B and George B K 2017 Two-dimensional titanium nitride (Ti2N) MXene: synthesis, characterization, and potential application as surface-enhanced raman scattering substrate *ACS Nano* **11** 8892–900

[73] Yang S *et al* 2018 Fluoride-free synthesis of two-dimensional titanium carbide (MXene) using a binary aqueous system *Angew. Chem.* **130** 15717–21

[74] Shi H *et al* 2021 Ambient-stable two-dimensional titanium carbide (MXene) enabled by iodine etching *Angew. Chem. Int. Ed.* **60** 8689–93

[75] Pinto D *et al* 2020 Synthesis and electrochemical properties of 2D molybdenum vanadium carbides—solid solution MXenes *J. Mater. Chem.* A **8** 8957–68

[76] Anasori B *et al* 2016 Control of electronic properties of 2D carbides (MXenes) by manipulating their transition metal layers *Nanoscale Horiz.* **1** 227–34

[77] Anasori B *et al* 2015 Two-dimensional, ordered, double transition metals carbides (MXenes) *ACS Nano* **9** 9507–16

[78] Handoko A D *et al* 2018 Tuning the basal plane functionalization of two-dimensional metal carbides (MXenes) to control hydrogen evolution activity *ACS Appl. Energy Mater.* **1** 173–80

[79] Wang L, Han M, Shuck C E, Wang X and Gogotsi Y 2021 Adjustable electrochemical properties of solid-solution MXenes *Nano Energy* **88** 106308

[80] Wang H *et al* 2022 Solid solution reinforced V3CrC3Tx MXene cathodes for Zn-ion micro-supercapacitors with high areal energy density and superior flexibility *J. Mater. Chem.* A **10** 20953–63

[81] Qin T, Wang Z, Wang Y, Besenbacher F, Otyepka M and Dong M 2021 Recent progress in emerging two-dimensional transition metal carbides *Nano-Micro Lett.* **13** 183

[82] Shacklette L W and Williams W S 1973 Influence of order-disorder transformations on the electrical resistivity of vanadium carbide *Phys. Rev.* B **7** 5041–53

[83] Lipatnikov V N, Lengauer W, Ettmayer P, Keil E, Groboth G and Kny E 1997 Effects of vacancy ordering on structure and properties of vanadium carbide *J. Alloys Compd.* **261** 192–7

[84] Natu V, Hart J L, Sokol M, Chiang H, Taheri M L and Barsoum M W 2019 Edge capping of 2D-MXene sheets with polyanionic salts to mitigate oxidation in aqueous colloidal suspensions *Angew. Chem. Int. Ed.* **58** 12655–60

[85] Wang B, Liu Y and Ye J 2013 Mechanical properties and electronic structures of VC, V_4C_3 and V_8C_7 from first principles *Phys. Scr.* **88** 015301

[86] Chen H, Ma H and Li C 2021 Host–guest intercalation chemistry in MXenes and its implications for practical applications *ACS Nano* **15** 15502–37

[87] Iqbal A, Hong J, Ko T Y and Koo C M 2021 Improving oxidation stability of 2D MXenes: synthesis, storage media, and conditions *Nano Converg.* **8** 9

[88] McDonnell F R M, Pink R C and Ubbelohde A R 1951 39. Some physical properties associated with 'aromatic' electrons. Part III. The pseudo-metallic properties of potassium–graphite and graphite–bromine *J. Chem. Soc.* **0** 191–7

[89] Mortimer R G 2008 *Physical chemistry* (Amsterdam, Boston: Academic) 3rd edn

[90] Dresselhaus M S (ed) 1986 *Intercalation in Layered Materials* 148 (Boston, MA: Springer US)

[91] Chong X, Jiang Y, Zhou R and Feng J 2014 Electronic structures mechanical and thermal properties of V–C binary compounds *RSC Adv.* **4** 44959–71

[92] Sun Z, Ahuja R and Lowther J E 2010 Mechanical properties of vanadium carbide and a ternary vanadium tungsten carbide *Solid State Commun.* **150** 697–700

[93] Jhi S-H, Ihm J, Louie S G and Cohen M L 1999 Electronic mechanism of hardness enhancement in transition-metal carbonitrides *Nature* **399** 132–4

[94] Liu Y, Jiang S P and Shao Z 2020 Intercalation pseudocapacitance in electrochemical energy storage: recent advances in fundamental understanding and materials development *Mater. Today Adv.* **7** 100072

[95] Wang C, Chen S and Song L 2020 Tuning 2D MXenes by surface controlling and interlayer engineering: methods, properties, and synchrotron radiation characterizations *Adv. Funct. Mater.* **30** 2000869

[96] Osti N C *et al* 2016 Effect of metal ion intercalation on the structure of MXene and water dynamics on its internal surfaces *ACS Appl. Mater. Interfaces* **8** 8859–63

[97] Liu F, Liu Y, Zhao X, Liu K, Yin H and Fan L-Z 2020 Prelithiated V2C MXene: a high-performance electrode for hybrid magnesium/lithium-ion batteries by ion cointercalation *Small* **16** 1906076

[98] Wang C, Chen S, Xie H, Wei S, Wu C and Song L 2019 Atomic Sn4 + decorated into vanadium carbide MXene interlayers for superior lithium storage *Adv. Energy Mater.* **9** 1802977

[99] Dusastre V (ed) 2011 *Materials for Sustainable Energy: a Collection of Peer-reviewed Research and Review Articles from Nature Publishing Group.* (Hackensack, NJ: World Scientific: Nature Pub. Group)

[100] Qi S *et al* 2019 Mesoporous carbon-coated bismuth nanorods as anode for potassium-Ion batteries *Phys. Status Solidi RRL —Rapid Res. Lett.* **13** 1900209

[101] Maradin D 2021 Advantages and disadvantages of renewable energy sources utilization *Int. J. Energy Econ. Policy* **11** 176–83

[102] Mohtasham J 2015 Review article-renewable energies *Energy Procedia* **74** 1289–97

[103] Rasheed T 2022 MXenes as an emerging class of two-dimensional materials for advanced energy storage devices *J. Mater. Chem.* A **10** 4558–84

[104] Eames C and Islam M S 2014 Ion intercalation into two-dimensional transition-metal carbides: global screening for new high-capacity battery materials *J. Am. Chem. Soc.* **136** 16270–6

[105] Wu M, He Y, Wang L, Xia Q and Zhou A 2020 Synthesis and electrochemical properties of V2C MXene by etching in opened/closed environments *J. Adv. Ceram.* **9** 749–58

[106] Whittingham M S 2004 Lithium batteries and cathode materials *Chem. Rev.* **104** 4271–302
[107] Das P and Wu Z-S 2020 MXene for energy storage: present status and future perspectives *J. Phys.: Energy* **2** 032004
[108] Gandla D, Zhang F and Tan D Q 2022 Advantage of larger interlayer spacing of a Mo2Ti2C3 MXene free-standing film electrode toward an excellent performance supercapacitor in a binary ionic liquid–organic electrolyte *ACS Omega* **7** 7190–8
[109] Yan B *et al* 2020 Oxygen/sulfur decorated 2D MXene V2C for promising lithium ion battery anodes *Mater. Today Commun.* **22** 100713
[110] Shi-Qiang W E I, Chang-Da W, Peng-Jun Z, Ke-Fu Z H U, Shuang-Ming C and Li S 2020 Mn 2^{+} intercalated V2C MXene for enhanced sodium ion battery *J. Inorg. Mater.* **35** 139
[111] Venkatkarthick R *et al* 2020 Vanadium-based oxide on two-dimensional vanadium carbide MXene (V2Ox@V_2CT_x) as cathode for rechargeable aqueous zinc-ion batteries *ACS Appl. Energy Mater.* **3** 4677–89
[112] Morphology restrained growth of V2O5 by the oxidation of V-MXenes as a fast diffusion controlled cathode material for aqueous zinc ion batteries - Chemical Communications (RSC Publishing) https://pubs.rsc.org/en/content/articlelanding/2020/c.c./d0cc01802c (accessed Apr. 27, 2022)
[113] Elia G A *et al* 2016 An overview and future perspectives of aluminum batteries *Adv. Mater.* **28** 7564–79
[114] Das S K, Mahapatra S and Lahan H 2017 Aluminium-ion batteries: developments and challenges *J. Mater. Chem.* A **5** 6347–67
[115] González A, Goikolea E, Barrena J A and Mysyk R 2016 Review on supercapacitors: technologies and materials *Renew. Sustain. Energy Rev.* **58** 1189–206
[116] Mashtalir O *et al* 2013 Intercalation and delamination of layered carbides and carbonitrides *Nat. Commun.* **4** 1
[117] Ruoff R 2008 Calling all chemists *Nat. Nanotechnol.* **3** 10–1
[118] Zhu J, Tang Y, Yang C, Wang F and Cao M 2016 Composites of TiO2 nanoparticles deposited on Ti3C2 MXene nanosheets with enhanced electrochemical performance *J. Electrochem. Soc.* **163** A785
[119] Shuang-Yan Lin and Xitian Zhang 2015 Two-dimensional titanium carbide electrode with large mass loading for supercapacitor *J. Power Sources* **294** 354–59
[120] Tang Y, Zhu J, Yang C and Wang F 2016 Enhanced capacitive performance based on diverse layered structure of two-dimensional Ti3C2 MXene with long etching time *J. Electrochem. Soc.* **163** A1975
[121] Wen Y *et al* 2017 Nitrogen-doped Ti3C2Tx MXene electrodes for high-performance supercapacitors *Nano Energy* **38** 368–76
[122] Liu J *et al* 2018 Advanced energy storage devices: basic principles, analytical methods, and rational materials design *Adv. Sci.* **5** 1700322
[123] Syamsai R and Grace A N 2020 Synthesis, properties and performance evaluation of vanadium carbide MXene as supercapacitor electrodes *Ceram. Int.* **46** 5323–30
[124] He H, Xia Q, Wang B, Wang L, Hu Q and Zhou A 2020 Two-dimensional vanadium carbide (V2CTx) MXene as supercapacitor electrode in seawater electrolyte *Chin. Chem. Lett.* **31** 984–7
[125] Zhang L, Zhang W-B, Zhang Q, Bao X and Ma X-J 2020 Electrochemical capacitance of intermetallic vanadium carbide *Intermetallics* **127** 106976
[126] Ming F *et al* 2019 Porous MXenes enable high performance potassium ion capacitors *Nano Energy* **62** 853–60
[127] Shuck C E *et al* 2020 Scalable synthesis of Ti3C2Tx MXene *Adv. Eng. Mater.* **22** 1901241